FDNS CFD Code Benchmark for RBCC Ejector Mode Operation: ContinuingToward Dual Rocket Effects

Jeff West and Joseph H. Ruf
Marshall Space Flight Center
Huntsville, Alabama 35812

ABSTRACT

Computational Fluid Dynamics (CFD) analysis results are compared with benchmark quality test data from the Propulsion Engineering Research Center's (PERC) Rocket Based Combined Cycle (RBCC) experiments to verify fluid dynamic code and application procedures. RBCC engine flowpath development will rely on CFD applications to capture the multi-dimensional fluid dynamic interactions and to quantify their effect on the RBCC system performance. Therefore, the accuracy of these CFD codes must be determined through detailed comparisons with test data. The PERC experiments build upon the well-known 1968 rocket-ejector experiments of Odegaard and Stroup [1] by employing advanced optical and laser based diagnostics to evaluate mixing and secondary combustion. The Finite Difference Navier Stokes (FDNS) code [2] was used to model the fluid dynamics of the PERC RBCC ejector mode configuration. Analyses were performed for the Diffusion and Afterburning (DAB) test conditions at the 200-psia thruster operation point. Results with and without downstream fuel injection are presented.

INTRODUCTION

The PERC RBCC test hardware began as a single rocket two-dimensional design (Figure 1) with variable geometry to enable studies of RBCC mixing and secondary combustion phenomena. Gaseous hydrogen and oxygen were used as rocket propellants with gaseous hydrogen injection at the end of the diffuser section for Diffusion and After-Burning (DAB) testing. Test measurements include wall static pressure, wall heat flux and overall thrust. Raman images taken during testing are used to obtain species mole fraction distributions for various stations downstream of the primary rocket to evaluate mixing and secondary combustion in the RBCC duct [3]. These measurements provide quality benchmark test data for CFD code validation. This paper compares the FDNS code results with the available benchmark test data.

The results presented here will be limited to the direct connect configuration under conditions of Case 3 which results in mass flow rates summarized in Table 1. For this case air is introduced into the inlet of the RBCC duct through a manifold and the duct contents are exhausted to the ambient environment through a converging nozzle. The primary rocket was designed to operate at 200 psia chamber pressure with an exit static pressure approximately equal to one atmosphere. This primary rocket is referred to as the single rocket-200 psia design or SR200. (Previous testing has used a single rocket-500 psia design (SR500) and future testing will involve twin rockets-200 psia design(TR200)) Two RBCC ducts nozzles were tested with the same primary thruster operating at 200 psia chamber pressure. The first had a 5 inch tall by 3 inch wide exit that was originally used for the cases with the primary thruster operating at 500 psia chamber pressure. The second RBCC duct nozzle's exit area was reduced by 40 percent (see Table 2) to increase duct pressure to improve the Raman spectroscopy measurements. These RBCC configurations are referred to as RBCC500 and RBCC200 respectively. At the time of this

writing, experimental data is available for the RBCC500 (with SR200) but is not available for the RBCC200.

APPROACH

All numerical analyses in this presentation modeled the DAB test. The rocket was run stoichiometric (O/F=8) at 200 psia chamber pressure. Simulations with and without fuel injected downstream of the rocket were performed. For cases in which it was included, fuel is injected in the afterburner section of the RBCC duct where the rocket exhaust and the entrained air are completely mixed. The first set of simulations modeled the RBCC500 duct configuration and the second set modeled the RBCC200 configuration. Flow rates for the FDNS simulations are given in Table 1.

All grids for the current analyses were generated with the software package Gridgen [4] using drawings supplied by PERC. A multizone 3D grid with 661,505 grid points was generated to model the RBCC duct flowpath. The grid includes the exit planes of the air inlet manifolds, the exit plane of the thruster, the exit planes of the fuel injection ports in the duct sidewall, and a portion of the ambient environment into which the duct exhausts. This domain models one quarter of the hardware flowpath and is relatively coarse in the third direction, depth. Solutions on more dense grids were conducted but the small improvements gained were deemed insignificant when compared to the substantial increase in required computational resources. All FDNS analyses were steady state and implemented finite-rate chemistry and thermodynamics with the compressibility-corrected extended k-ε turbulence model. The current chemistry model includes 7 species (H_2, O_2, H_2O, H, O, OH, and N_2) and 9 chemical reactions. N_2 is considered inert while all other species are considered to be reactive. Results were computed on both a multiprocessor SGI Power Challenge and a 4-node, 8-CPU Beowulf PC Cluster.

In each case, the ejector mode analysis treats the rocket exit as a fixed inlet with the mass flow rate matching that of the corresponding PERC test. Additionally, the fuel injection ports in the DAB case were treated as fixed inlets. All walls are treated as no-slip adiabatic surfaces. A total pressure of one atmosphere is conserved on the far field freestream boundaries and symmetry conditions used along symmetry boundaries.

The primary rocket exit flow conditions for the DAB cases were obtained from a separate rocket-only calculation using FDNS and a 220,211 grid point grid constructed from drawings supplied by PERC. The rocket computational domain covered the one-quarter symmetry as in the main duct analysis. The same chemical kinetic mechanism as in the main duct was used for the rocket. Rocket inlet plane properties were calculated using the CEC Chemical equilibrium code under the pressure and O/F given in Table 1. Supersonic exit boundary conditions were used at the nozzle exit and symmetry boundary conditions were used on symmetry planes. The no-slip wall temperature boundary conditions from a previous study[5] of the 500-psia counterpart to this primary rocket.

RESULTS AND DISCUSSION

RBCC 500 Case

FDNS calculated pressure and measured static pressure with fuel injection (Ram-On) are compared in Figure 2. The primary rocket nozzle exit is located at x=0.0 inches. The computed results over-predict the static pressure for x<0 by as much as 0.8 psia. The experimental results show an earlier rise in static pressure than do the computed results. Near the location of the fuel injection (x=70 inches), the computed results over-predict the pressure by approximately 0.25 psia.

FDNS calculated pressure and measured static pressure without fuel injection (Ram-Off are compared in Figure 3. While these results show a uniform drop in pressure throughout the duct, the computed results still over-predict the static pressure for x<0 by as much as 0.8 psia. The earlier rise in static pressure than computed results and the over-prediction of the downstream pressure by the computed results are still present.

Over-prediction of pressure by approximately the same magnitude for x<0 is evident in previous comparisons of direct connect simulations and experimental data [5]. A systematic omission in the computational model is the airbox flow straighteners, which consists of two 1/8 inch thick plates with 3/16 inch diameter drilled holes spaces at 5/16 inch intervals with staggered rows such that equilateral triangles are formed by the hole centers. This configuration results in 32 percent open area for each plate.

It may be that inclusion of this flow straighening device enhances the effect of the ejector, allowing the "pumping down" of the pressure downstream of the flow straighteners. This lowered pressure in the computed results would tend to result in a greater angle of expansion of the supersonic thruster exhaust, earlier attachment of the flow to the duct wall, and better agreement with experiment. The FDNS CFD code has a porosity capability with which to model the two perforated plates. This possibility will be the subject of investigation in the near future.

H_2O, O_2, N_2, and H_2, mole fractions for RBCC500 with afterburner injection are shown on the left-hand side of Figure 4 for four axial locations, x=2.3, 6.3, 9.3, and 13.3 inches respectively. Results are presented where x is the axial distance downstream of the thruster exit plane and the vertical position in the RBCC duct. Note that the orientation of this figure is such that the flow direction is from bottom to top. The mixing is nearly complete by the x=13.3 inch station.

RBCC 200 Case

FDNS calculated static pressures with and without downstream fuel injection for the RBCC200 duct are presented in Figure 5 along with the corresponding pressures for the RBCC500 duct. The reduction in exit area increased the static pressure in the duct substantially, to the same range of pressures where Raman data was acquired previously. Experimental data is not yet available to compare with these results. However, from Figure 5 it is evident that the RBCC200 duct design results in a more aggressive pressure rise downstream of the primary rocket. H_2O, O_2, N_2, and H_2, mole fractions are shown on the right-hand side of Figure 4 at the same locations as for the RBCC500 simulation. The mixing is seen to be significantly more complete for the RBCC200 duct than for the RBCC500 duct.

Understanding of the reasons for the quicker mixing and pressure rise can be gained by the comparison of the computed results from previous results [6] with the present results. Density, selected streamlines, and static temperature distributions along the symmetry plane are compared for three cases in Figure 6. The one-quarter geometry was mirrored about the x-axis to present a one-half symmetry view. In each view, the variable above the centerline is density and streamlines, and the variable below the centerline is static temperature.

The top view is the previously reported [6] results of the SR500 primary rocket operating at 500 psia and a flow rate of 0.6796 lbm/s at an O/F of 8.0 exhausting into the RBCC500 duct. The air flow rate is 1.56 lbm/sec and the downstream fuel injection rate is 0.0455 lbm/sec and the duct O/F is 8.0. The middle view is the current SR200 rocket with Table 1 operating conditions exhausting into the RBCC500 duct. The bottom view is the SR200 rocket with Table 1 operating conditions exhausting in to the RBCC200 duct.

Attachment of the thruster plume to the top wall is delayed the most for the top case. The middle case attaches earlier than the top case and a recirculation zone is present upstream of the attachment point. The vertical temperature gradient is a result of the recirculation and not from a flame front. The bottom case attaches very quickly with a very vigorous three-dimensional recirculation zone. This recirculation zone penetrates upstream farther near the duct wall and even penetrates slightly upstream of the thruster nozzle exit.

CONCLUSIONS

Results of modeling the PERC RBCC test article under Direct Connect Case 3 conditions with the FDNS CFD code has been presented. Comparisons of computed and experimental duct pressure profiles for 200 psia primary rocket operation with and without downstream fuel injection has been presented. The computed results are in fair agreement with experimental results. The computed changes in mixing and wall attachment tendencies of the primary rocket plume for changes in primary rocket pressure and flow rate, and duct flow rate and geometry have been illustrated. Future modeling refinements include modeling of the air straightening devices.

REFERENCES

[1] Odegaard, E. A. and Stroup, K. E., "1966 Advanced Ramjet Concepts Program, Volume VIII-Ejector Ramjet Engine Tests- Phase I", The Marquardt Corporation, Technical Report AFAPL-TR-67-118, Volume VIII, January 1968.

[2] Chen, Y. S., "FDNS - A General Purpose CFD Code, Version 4.0", Engineering Sciences, Inc., ESI-TR-97-01, Huntsville, AL., May 1997.

[3] Lehman, M., Pal, S., Broda, J. C. and Santoro, R. J., "Raman Spectroscopy Based Study of RBCC Ejector Mode Performance," AIAA-99-0090, 37th AIAA Aerospace Sciences Meeting, Reno, NV, January 11-14, 1999.

[4] Gridgen Version 13 user manual, http://pointwise.com/

[5] Pal, S., Tucker, K., Lehman, M., and Santoro, R., "Experimental Studies of Heat Transfer in Rectangular Nozzles for CFD Design Methodology", 33rd ASME/AiChE/ANS/AIAA National Heat Transfer Conference, August 15-17, 1999, Albuquerque, New Mexico.

[6] Ruf, J. H., "Benchmark of FDNS CFD Code For Direct Connect RBCC Test Data", AIAA 2000-3726, 36th AIAA/ASME/SAE/ASEE Joint Propulsion Conference, 16-19 July, 2000, Hunstville, AL.

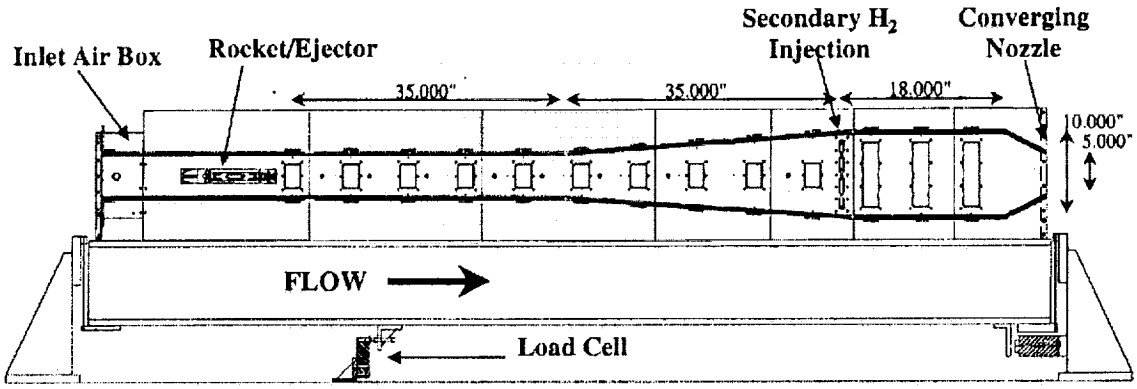

Figure 1. PERC RBCC ejector mode experimental hardware (RBCC500 configuration)

Table 1 FDNS CFD Run Conditions for Case 3

	Ram-On	Ram-Off
Rocket O/F	8	8
Rocket GO_2 (lbm/sec)	0.243	0.243
Rocket GH_2 (lbm/sec)	0.0304	0.0304
Rocket P_c (psia)	200	200
Air injection (lbm/sec)	0.63	0.63
GH_2 afterburner injection (lbm/sec)	0.0183	0.0
O/F between GO_2 in Air and GH_2 in duct	8.0	-

Table 2 RBCC Duct Exhaust Geometry Details

	RBCC500	RBCC200
Exhaust Width (inches)	3	3
Exhaust Height (inches)	5	2
Exhaust Convergence Half-Angle (degrees)	45	45
Duct Exit Plane Location with respect to thruster nozzle exit (inches)	93	96

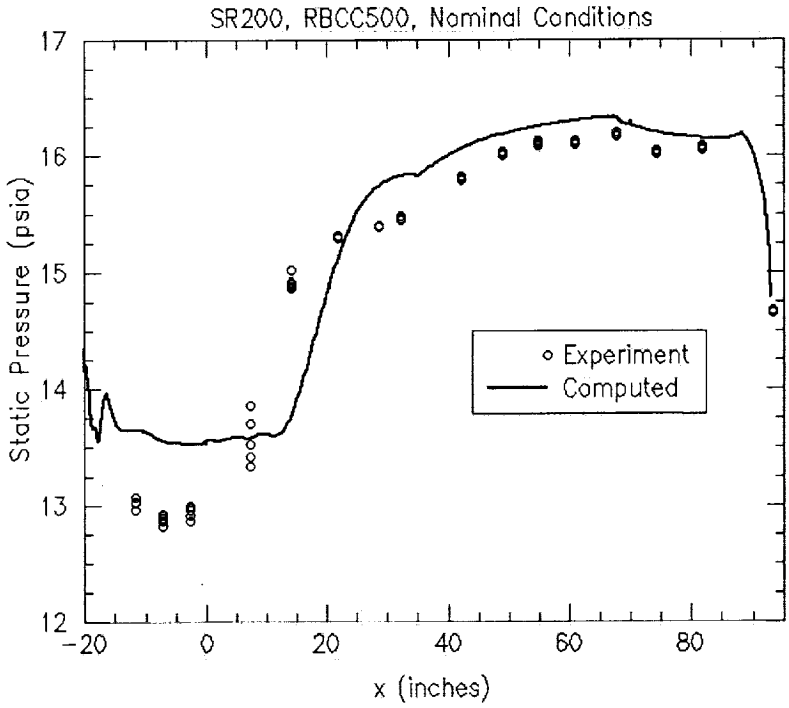

Figure 2. Axial top wall static pressure comparison with downstream fuel injection

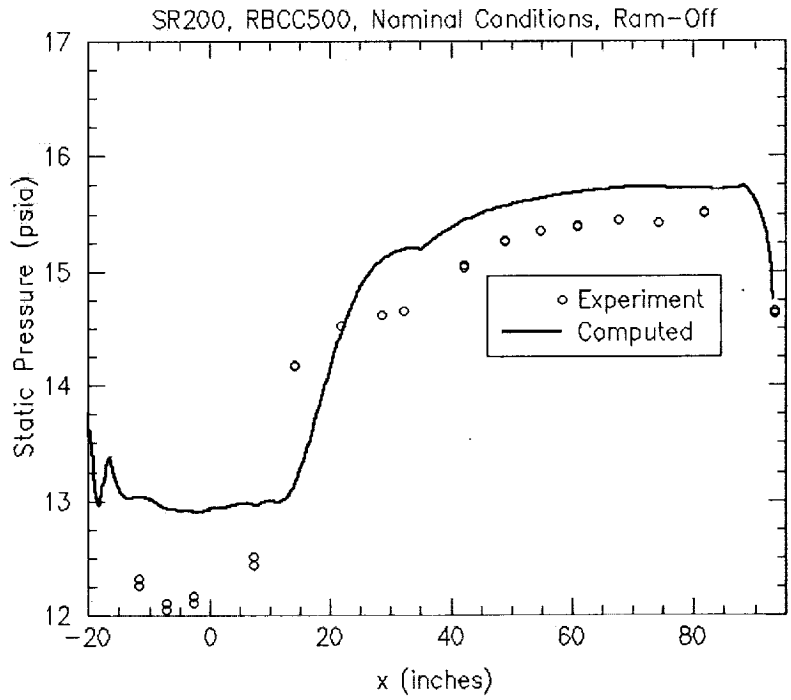

Figure 3. Axial top wall static pressure comparison without downstream fuel injection

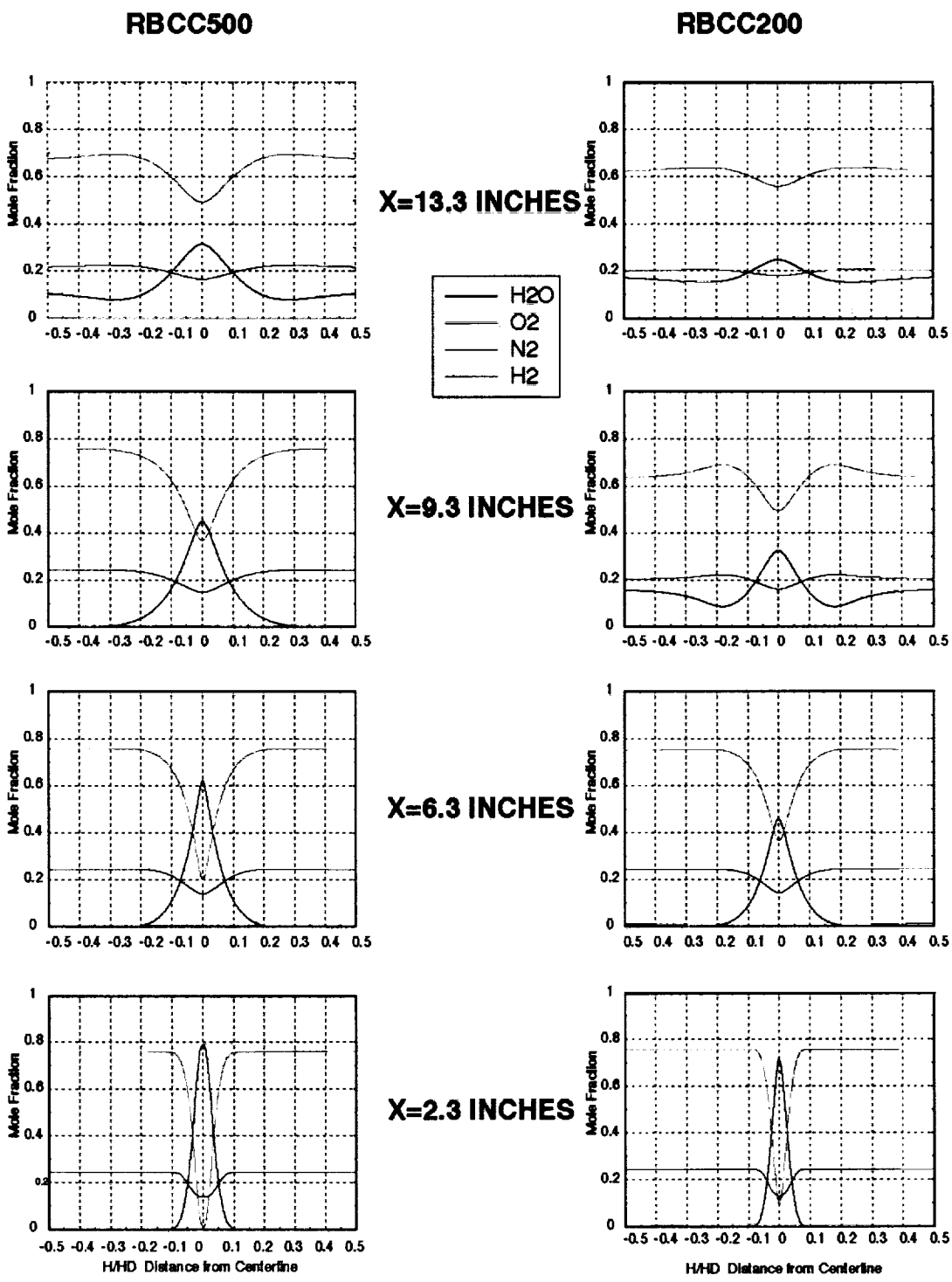

Figure 4. Species mole fraction (N_2, O_2, H_2O, and H_2) comparison for the RBCC500 (left) and RBCC200 (right) designs. Profiles are located at x=2.3, 6.3, 9.3, and 13.3 inches downstream of thruster exit.

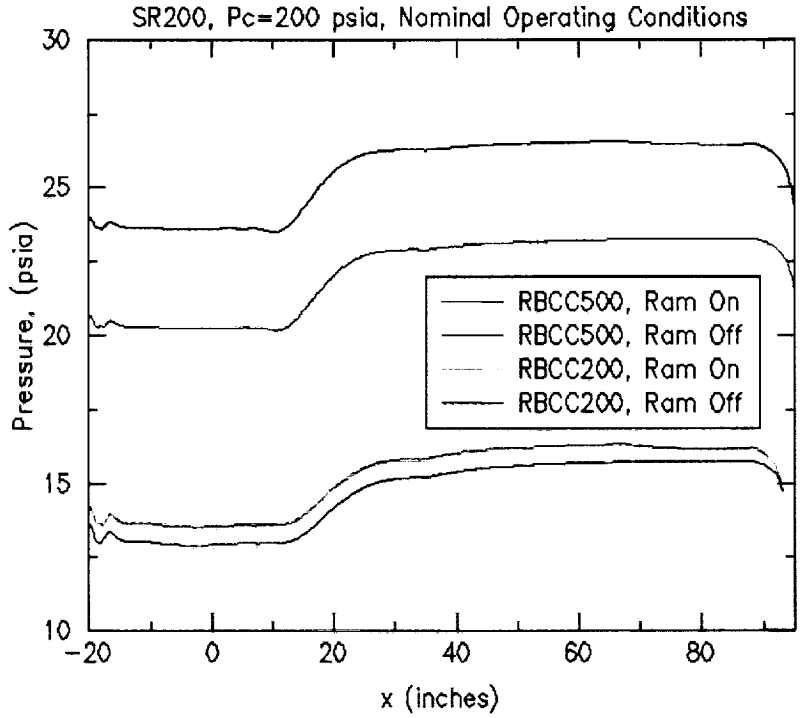

Figure 5. Comparison of top wall static pressure profiles.

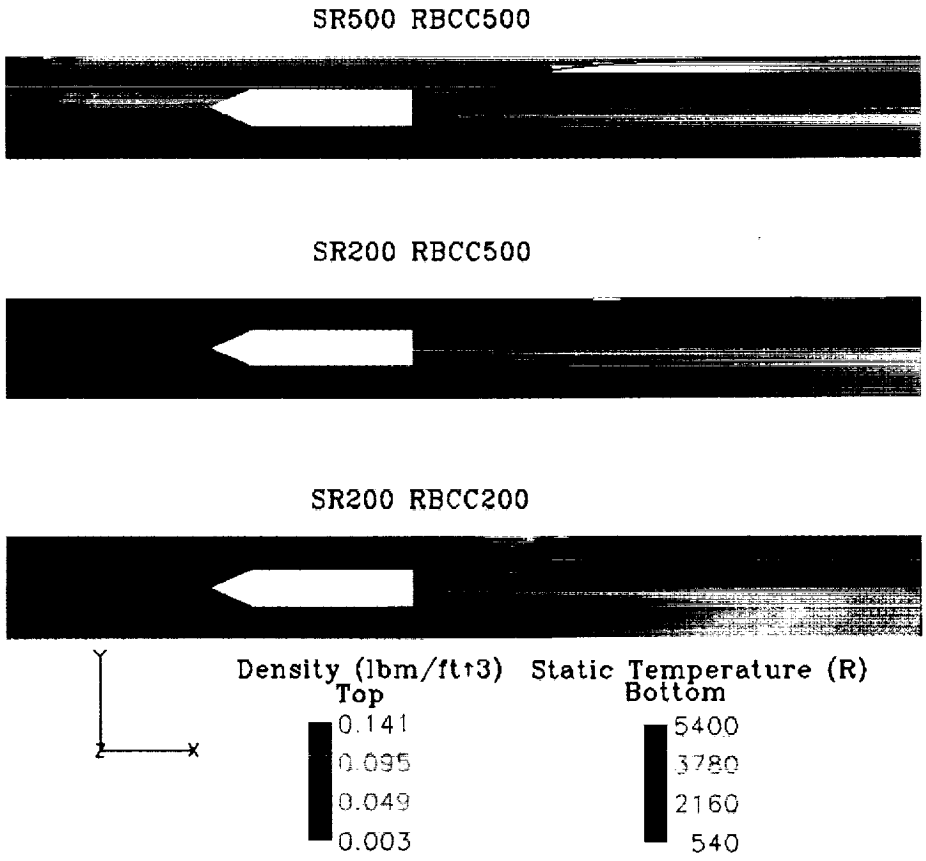

Figure 6. Comparison of mixing region between three cases.